Nanomed J. 12(2): 324-334, Spring 2025

RESEARCH PAPER

Synthesis of PLGA nanoparticles containing Auraptene and evaluation of their anti-cancer effects

Suha Lefta bedan [1], Ali Es-haghi [2], Hadi Zare-Zardini [3]*

[1]Department of Biology, Science and Research Branch, Islamic Azad University (IAU), Tehran, Iran
[2]Department of Biology, Mashhad Branch, Islamic Azad University, Mashhad, Iran
[3]Department of Biomedical Engineering, Meybod University, Meybod, Iran

ABSTRACT

Objective(s): Cancer remains a leading cause of mortality globally, necessitating novel and effective therapies. Nanotechnology, particularly poly (lactic-co-glycolic acid) (PLGA) nanoparticles, offers promising potential for safe and effective delivery of therapeutic agents due to their biocompatibility, biodegradability, and tunable release properties. This study aimed to synthesize PLGA nanoparticles loaded with auraptene (Aur-PLGA-NPs) and evaluate their anti-cancer effects.

Materials and Methods: Aur-PLGA-NPs were synthesized and characterized using particle size analyzer, transmission electron microscopy (TEM), field emission scanning electron microscopy (FESEM), X-ray diffraction (XRD), and Fourier transform infrared (FTIR). Cytotoxic effects were assessed against HT-29 colon cancer cells and human umbilical vein endothelial cells (HFF) as normal controls. Apoptotic mechanisms were investigated through 4,6-diamidino-2-phenylindole (DAPI) staining, flow cytometry, and gene expression analysis of caspase-3, caspase-9, and BAX.

Results: Spherical nanoparticles with an average size of 185 nm were successfully synthesized. Aur-PLGA-NPs exhibited higher cytotoxicity against HT-29 cancer cells compared to HFF normal cells. Furthermore, Aur-PLGA-NPs significantly enhanced the expression of apoptotic genes caspase-3, caspase-9, and BAX in HT-29 cells.

Conclusion: The increased cytotoxicity of Aur-PLGA-NPs against cancer cells suggests their potential as anti-cancer agents. However, further studies are needed to evaluate their effects on other cancer cell lines and elucidate the underlying anti-cancer mechanisms.

Keywords: *Auraptene, Antineoplastic agents, Nanoparticles, Poly(lactic-co-glycolic acid)*

How to cite this article
Lefta bedan S, Es-haghi A, Zare-Zardini H. Synthesis of PLGA nanoparticles containing Auraptene and evaluation of their anti-cancer effects. Nanomed J. 2025; 12(2): 324-334. DOI: 10.22038/nmj.2024.79422.1958

INTRODUCTION

Cancer continues to be a major global health concern. Every year, millions of people are diagnosed with cancer, and many of them die from the disease [1, 2]. Conventional cancer therapies, such as chemotherapy and radiation, are often associated with significant side effects and limited efficacy [3]. Therefore, there is a continuous search for novel therapeutic approaches with more effectiveness, less toxicity, and minimal adverse effects [4].

Nanoparticle-based drug delivery systems have emerged as a promising strategy for cancer treatment [5]. These systems offer numerous advantages, including enhanced drug stability, controlled release, improved bioavailability, and targeted delivery to tumor tissues [6-9]. Among various types of nanoparticles, poly (lactic-co-glycolic acid) (PLGA) nanoparticles have gained significant attention due to their biocompatibility, biodegradability, and versatility in encapsulating a wide range of therapeutic agents [10, 11].

The use of natural products in the synthesis of nanoparticles offers various advantages, including reducing side effects in the treatment of various diseases such as cancer [12, 13]. Auraptene, a natural compound found in various citrus fruits, has attracted attention in recent years due to

* *Corresponding author: Emails: ashaghi@gmail.com; eshaghi5510@mshdiau.ac.ir*
Note. This manuscript was submitted on April 19, 2024; approved on August 11, 2024

its potential anticancer properties [14, 15]. Preclinical studies have shown that auraptene exhibits antiproliferative, proapoptotic, and anti-metastatic effects on various cancer cell lines and tumor-bearing animal models. However, the clinical application of auraptene is hindered by its low solubility and poor bioavailability [16].

The encapsulation of auraptene into PLGA nanoparticles can provide an effective solution to overcome these limitations. The formulation of PLGA nanoparticles allows for the controlled release of auraptene, improving its bioavailability and enhancing its therapeutic efficacy. Furthermore, PLGA nanoparticles can be functionalized to target specific cancer cells or tissues, thereby increasing the selectivity of loaded drugs and minimizing their off-target delivery.

The use of PLGA nanoparticles as a drug delivery system offers several advantages in cancer treatment. First, the biocompatible and biodegradable nature of PLGA ensures its biosafety and rapid elimination from the body after drug release [17]. Second, the controlled release of auraptene from PLGA nanoparticles allows for sustained drug release at the target site, increasing its therapeutic efficacy. Third, the versatility of PLGA nanoparticles enables the incorporation of targeting ligands or surface modifications to improve their specificity and selectivity towards cancer cells [18]. Therefore, auraptene-loaded PLGA nanoparticles offer a promising approach for cancer treatment. Overall, nano-based drug delivery systems offer numerous advantages, including improved drug stability, controlled release, enhanced bioavailability, and targeted delivery [19-21].

The objective of this study was to synthesize PLGA nanoparticles and encapsulate them with auraptene. Our secondary aim was to evaluate the anti-cancer effects of auraptene-loaded PLGA nanoparticles (Aur-PLGA-NP) *in-vitro* against HT-29 cancer cells. Finally, the potential mechanisms of the anti-cancer effects of Aur-PLGA-NPs were investigated. Auraptene encapsulation into PLGA nanoparticles is expected to improve its stability, solubility, and cellular uptake, leading to better therapeutic outcomes. The results of this study can contribute to the development of more effective and less toxic cancer treatment strategies, which ultimately can improve the outcomes of cancer patients.

MATERIALS AND METHODS

Materials

Propidium iodide (PI), 3,4,5-Dimethylthiazol-2-yl-2,5-diphenyltetrazolium bromide (MTT), and fetal bovine serum (FBS) were procured from Sigma-Aldrich. The culture medium and penicillin-streptomycin were purchased from Invitrogen. SYBR green and cDNA synthesis kits were from Qiagen. The HT-29 (colon cancer) and HFF cell lines were from the Bu-Ali Research Institute (Iran).

Synthesis of Aur-PLGA-NPs

The synthesis of Aur-PLGA-NPs was conducted using the single emulsion solvent evaporation method [22]. Initially, a solution of PLGA in dichloromethane (DCM) was prepared at a specified concentration. Auraptene was then dissolved in this organic phase. The organic phase containing PLGA and auraptene was slowly poured into an aqueous phase consisting of polyvinyl alcohol (PVA) at a concentration of 2% w/v, while stirring continuously at a rate of 600 rpm to ensure proper dispersion. The emulsion was homogenized using a high-pressure homogenizer at 10,000 psi for 10 cycles to achieve a fine and stable emulsion. Following homogenization, an additional 10 mL of 0.1% w/v PVA solution was introduced to the emulsion to facilitate the solvent evaporation process. The emulsion was then stirred at room temperature (approximately 25°C) for 120 min to allow the DCM to evaporate completely, leaving behind the PLGA nanoparticles encapsulating Aur. After the solvent evaporation step, the emulsion was centrifuged at 15,000 rpm for 30 min at 4 °C to separate the nanoparticles from the aqueous phase. The resulting pellet, containing the hybrid nano-formulation, was washed with distilled water to remove any residual PVA and unencapsulated Aur. The washed nanoparticles were then lyophilized using a freeze-dryer for 48 hr to obtain a dry powder of Aur-PLGA-NPs.

Characterization of Aur-PLGA-NPs

The techniques used for analyzing the specifications of Au-PLGA-NPs included Fourier Transform Infrared Spectroscopy (FTIR), transmission electron microscopy (TEM), dynamic light scattering (DLS), and Zeta potential analysis. In the range of 4000–400 cm^{-1}, the chemical groups of the hybrid system were screened using Fourier Transform Infrared (FTIR) spectroscopy. The PDI and size of Au-PLGA-NPs (mean diameter) were assessed by the DLS technique (Nano-ZS, Malvern, UK). The stability of the NPs was estimated based on Zeta potential assessment (Nano-ZS, Malvern,

UK). Finally, the morphology of the NPs was observed by TEM (JEOL, Tokyo, Japan).

Encapsulation efficiency and loading capacity

To assess the encapsulation percentage of Aurapten in PLGA, initial concentrations of auraptene were prepared, and the absorbance of each concentration was recorded at a wavelength of 320 nm using a UV-vis spectrophotometer (UV160-Shimadzu, Japan), from which a standard curve was derived. Subsequently, 1 mL of the Aur-PLGA-NPs supernatant was measured at 320 nm to quantify the nanocarrier encapsulation. The encapsulation efficiency and loading capacity of Aurapten were determined using the following equations:

$$\text{encapsulation efficiency}(\%) = \frac{\text{Mass of initial Auraptene} - \text{Mass of free Auraptene}}{\textit{Mass of initial}\ \text{Auraptene}} \times 100$$

$$\text{loading capacity}(\%) = \frac{\text{Mass of total entrapped auraptene}}{\textit{Mass of PLGA}} \times 100$$

***In-vitro* drug release**

To investigate the release kinetics of AUR from PLGA under physiological conditions, 5 mg of AUR-PLGA-NPs were dissolved in 5 mL of PBS at pH 7.4, sealed in a dialysis bag (MWCO = 3.5 kDa), and then dialyzed against 30 mL of PBS. For comparison, a control dialysis bag contained an equivalent concentration of free auraptene solution. The dialysis bags were subjected to magnetic stirring at 37 °C to simulate physiological conditions. At various time intervals, 500 µL of the solution was extracted from each bag and replaced with an equal volume of fresh PBS. The concentrations of aurapten in the samples were determined using UV-visible spectroscopy at a wavelength of 320 nm.

Cell culture and cytotoxicity analysis

Both cell lines (HT-29 and HFF) were grown in Roswell Park Memorial Institute (RPMI) 1640 medium containing FBS (10%) and antibiotics (penicillin-streptomycin, 1%). The basic culture medium was RPMI. The cells were seeded in 96-well plates for cytotoxicity analysis using the MTT reagent. For this purpose, the different concentrations (125, 250, and 500 µg/mL) of Aur-PLGA-NPs were used to treat the cell lines for 24 and 48 hr. The MTT reagent was added to the cells after the elimination of the culture medium. The experiment was continued by adding dimethyl sulfoxide (DMSO) (100 µL) reading absorbance (570 nm) to calculate cellular viability as follows:

Cell viability %= (sample absorbance/control absorbance) × 100

DAPI staining for apoptosis evaluation

Cancer cells were initially grown for 24 hr in RPMI (10% FBS and 1% antibiotic supplemented) in 6-well plates. Treatment with Aur-PLGA-NPs was conducted at the doses of 125, 250, and 500 µg/mL. After incubation and removal of the supernatant, the cells were fixed with methanol (1 mL, 70% v/v). Then, the cells were washed using PBS before the addition of the DAPI reagent. The cells were exposed to this dye for 15 min at 25.

Finally, the appearance of nuclei was assessed via fluorescent microscopy (Olympus DP27, Tokyo, Japan).

Apoptosis analysis by flow cytometry

After seeding and exposing HT-29 cancer cells to 125, 250, and 500 µg/mL of Aur-PLGA-NPs, they were subjected to Annexin V-FITC staining and evaluated by flow cytometry. For this purpose, we purchased a specialized kit from Abcam (ab14085). The cells exposed to the NPs were precipitated by centrifugation, and after eliminating the top layer containing culture media, the Binding Buffer 1X (0.5 mL) was added to the pellet. Finally, 5 µL of each of annexin V and propidium iodide (PI) was added to the cell suspension. After incubation for five minutes at dark, the percentage of necrotic and apoptotic cells were determined by flow cytometry.

Apoptotic genes' expression

The cancerous cells exposed to Aur-PLGA-NPs for 48 hr at the doses of 125, 250, and 500 µg/mL were harvested for RNA extraction (Rx BON kit) and subsequent gene expression assessment. Cellular RNA was extracted by initially degrading cell membranes (1 µL of lysis buffer), followed by chloroform addition (250 µL), 25incubation (15 min), and cold centrifugation (12,000 rpm, 4 °C, 15 min). At this step, the supernatant was collected and mixed with cold propanol (600-800 µL). After remaining at -20 °C for 24 hr, the cell suspensions were centrifuged (12,000 rpm, 4 °C, 45 min). Finally, 1000 µL of cold ethanol (70%) was added to the pellet, followed by centrifugation at 4 °C (12,000 rpm, 20 min). The final pellet was allowed to be dried at room condition, and RNA was dissolved in RNase-free distilled water at the final volume of 20 µL before being frozen at -80

°C. The purity and quantity of the extracted RNA were assessed by a Nano-Drop device. Using the Epoch device, 1 µL of RNA extracted was used for complementary DNA production using a Pars Tous kit (Iran) providing the reverse transcriptase enzyme. The manufacturer-provided buffer (10 µL) and transcriptase enzyme (2 µL) were mixed with deionized distilled water (8 µL). After 10 min of rotating on a vortex at 25 °C, the reaction mixture was transferred to 47 °C and incubated for 1 hr. The final phase of the reaction included incubation at 85 °C for 5 min. The cDNA generated was stored at -20 °C until being utilized in PCR for gene expression quantification. SYBR Green (10 µL), primers (1 µL of each of forward and reverse), distilled water (7 µL), and cDNA (1 µL) constituted PCR reaction components. Amplification was accomplished by the following thermal program: a single primary step at 95 °C for 15 min and 39 cycles of 95°C (15 sec), 59 °C (20 sec), and 72 °C (20 sec).

Statistical analysis

Data analysis was performed using descriptive statistics to calculate the mean and standard deviation (SD) for each group. Graphs were generated to visually represent the data, and statistical significance was determined using one-way analysis of variance (ANOVA) tests. All statistical procedures were conducted using SPSS software (version 20, IBM Corp., Armonk, NY, USA). Additionally, for the MTT assays, flow cytometry analysis, and other biological assays, the data were analyzed using GraphPad Prism software (San Diego, CA, USA). A P value less than 0.05 was considered statistically significant.

RESULTS AND DISCUSSIONS

Characterization of Au-PLGA-NPs

The synthesis of PLGA NPs containing auraptene holds significant potential for the development of novel anti-cancer therapies. Auraptene is a natural compound derived from citrus fruits, and it has shown promising anti-cancer properties in various studies [23]. The encapsulation of auraptene into the PLGA NPs offers several advantages, including the enhanced stability, controlled release, and improved cellular uptake of the drug. In this study, we successfully synthesized PLGA nanoparticles loaded with auraptene (Aur-PLGA-NP**)**. The successful synthesis of Aur-PLGA-NP was confirmed by various characterization techniques, including DLS (for size and zeta potential analysis), TEM (for morphology examination), and FTIR (for chemical characterization). The average size of Aur-PLGA-NPs was 185.79 nm (Fig. 1).

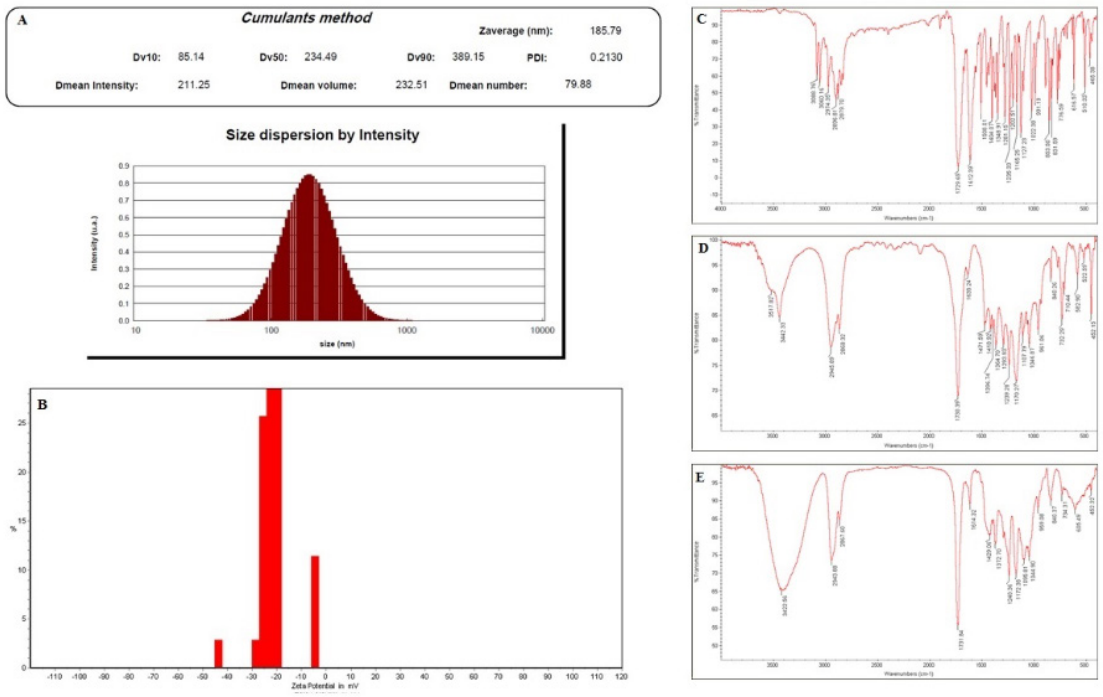

Fig. 1. A. DLS plot of Aur-PLGA-NPs. The average size of the particles was 185.79 nm, and PDI was equal to 0.2130. B) Zeta potential of Aur-PLGA-NPs. The zeta potential was obtained as -20 mV. The results confirmed the suitable formation of Aur-PLGA-NPs. C) FTIR spectrum of Aur. D) FTIR spectrum of PLGA-NPs. E) FTIR spectrum of Aur-PLGA-NPs.

As an index for size uniformity, PDI of the nanoparticles was calculated (PDI=0.21). A lower PDI generally indicates more homogeneity in shape and higher stability of NPs during storage. Regarding the relatively low PDI value of Aur-PLGA-NPs, we can conclude that these particles had acceptable morphological uniformity. The numerical range of PDI varies from 0 (indicating monodisperse particles) to 1 (reflecting polydisperse particles) [24]. In another study, nanoemulsions with low PDI showed acceptable size uniformity and prolonged stability during storage [25]. Likewise, lower PDIs and smaller particle sizes were noted to predict better brownian movements and diffusional patterns and lower sedimentation and creaming in nanoemulsions [26].

Zeta potential is one of the important factors to evaluate the stability of colloids [27, 28]. The Zeta potential of Aur-PLGA-NPs was recorded as -18.21 mV, confirming the stability of the hybrid system (Fig. 1b). The repulsion force between particles is somehow determined by their surface similarly charged molecules, a feature that is reflected by Zeta potential. Through facilitating inter-molecule and inter-particle interactions via surface charged molecules, Zeta potential has been noted to be important for the stability of nanoemulsions. Generally, kinetically stable nanoformulations possess a Zeta potential around ±30 mV. In a study, Zeta potential of -9.42 mV was reported to represent nanoemulsions with stable electrostatic behaviors [29]. In fact, the presence of similarly changed groups on the surface of nanoemulsions could prevent them from forming aggregates during storage [30]

The FTIR spectrum of Aur exhibited characteristic absorption bands at approximately 1729 cm^{-1}, which corresponds to the C=O stretching of the carbonyl group. Peaks observed around 1600-1620 cm^{-1} were attributed to C=C stretching, indicating the presence of conjugated double bonds in the aromatic ring structure. Additional peaks were observed at 12350 cm^{-1} and 1022 cm^{-1}, which can be attributed to the C–O stretching and C–C stretching vibrations, respectively. These functional groups are crucial for the biological activity of Aur. The FTIR spectrum of PLGA nanoparticles showed a strong absorption band around 1730 cm^{-1}, indicative of the C=O stretching vibrations associated with the ester functional groups in the polymer backbone. A peak at 1170 cm^{-1} was observed, corresponding to the C–O stretching vibrations, further confirming the polymeric nature of PLGA. The characteristic peaks of PLGA were consistent with the expected structure of the copolymer composed of lactic and glycolic acid units. The FTIR spectrum of Aur-PLGA-NP showed that the 3422.56 cm^{-1} band was related to N-H bonds. Also, the 2943.88 cm^{-1} and 1731 cm^{-1} bands in the spectrum were related to the phenyl ring (Fig. 1c). The FTIR spectrum confirmed the presence of auraptene within PLGA nanoparticles as evidenced by detecting characteristic peaks associated with both compounds. These analyses confirmed the formation of nanoparticles with a uniform size distribution suitable for drug delivery applications.

Examining the results of TEM and FESEM demonestrated that Aur-PLGA-NPs had a quasi-spherical appearance (Fig. 2A &B). The encapsulation efficiency and loading capacity of Aur-PLGA-NPs were 82.7% and 16.4%, respectively.

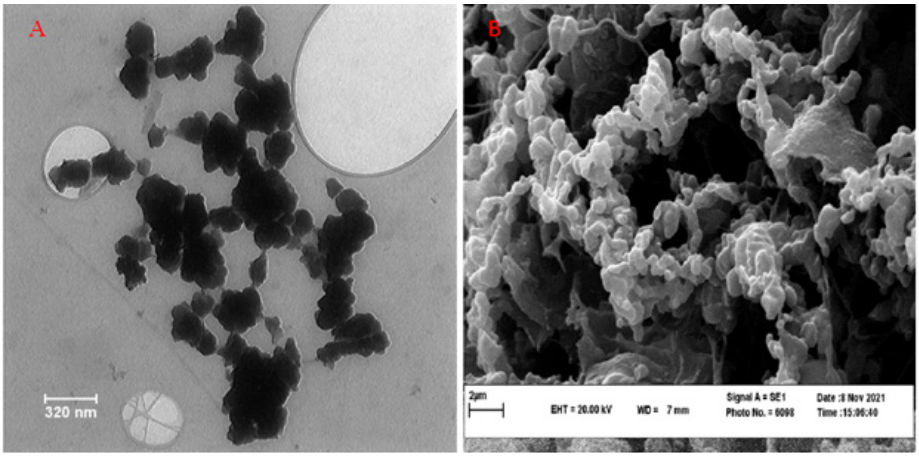

Fig. 2. TEM image (A) and FESEM image (B) of Aur-PLGA-NPs revealed that the particles were morphologically quasi-spherical

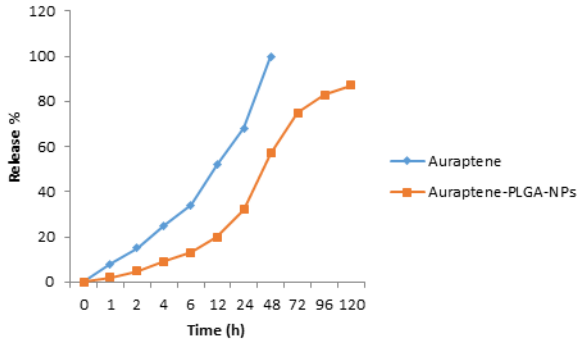

Fig. 3. *In-vitro* drug release profile of AUR-PLGA-NPs

In-vitro drug release profile of AUR-PLGA-NPs

The results demonstrated a sustained release of Aur from the PLGA nanoparticles compared to the free auraptene solution (Fig. 3). The slope of the release profile for the encapsulated Aur-PLGA-NPs was shallower compared to that of the free Aur solution, indicating a slower and more controlled release from the nanostructure. This slower release rate suggests that Aur is being released gradually from the PLGA nanoparticles and diffusing out of the dialysis membrane at a reduced rate compared to the free drug. The cumulative release profile indicated that the encapsulated Aur exhibited a slower and more controlled release over time. This slow release of Aur from the PLGA nanoparticles supports the hypothesis that encapsulation within the nanostructure can reduce the immediate toxicity of the substance by providing a more gradual release, which could potentially minimize adverse effects on normal cells *in-vivo.* This finding of controlled and sustained release from PLGA-based formulations aligns with the previous studies demonstrating the efficacy of PLGA as a delivery vehicle for various encapsulated agents [31-33].

Cytotoxicity of Aur-PLGA-NPs

Cell toxicity test by MTT method is one of the most is one of the most used techniques in the study of toxicology [34-36]. The anti-cancer effects of Aur-PLGA-NPs, as a crucial aspect of this study, were assessed *in-vitro* against a colon cancer cell line (HT-29). The nanoparticles exhibited a dose-dependent cytotoxic effect on the cancer cells, as demonstrated by the MTT assay. The IC_{50} value of auraptene-loaded PLGA nanoparticles was significantly lower against cancerous cells compared to normal cells.

Fig. 4A shows the cytotoxicity pattern of Aur-

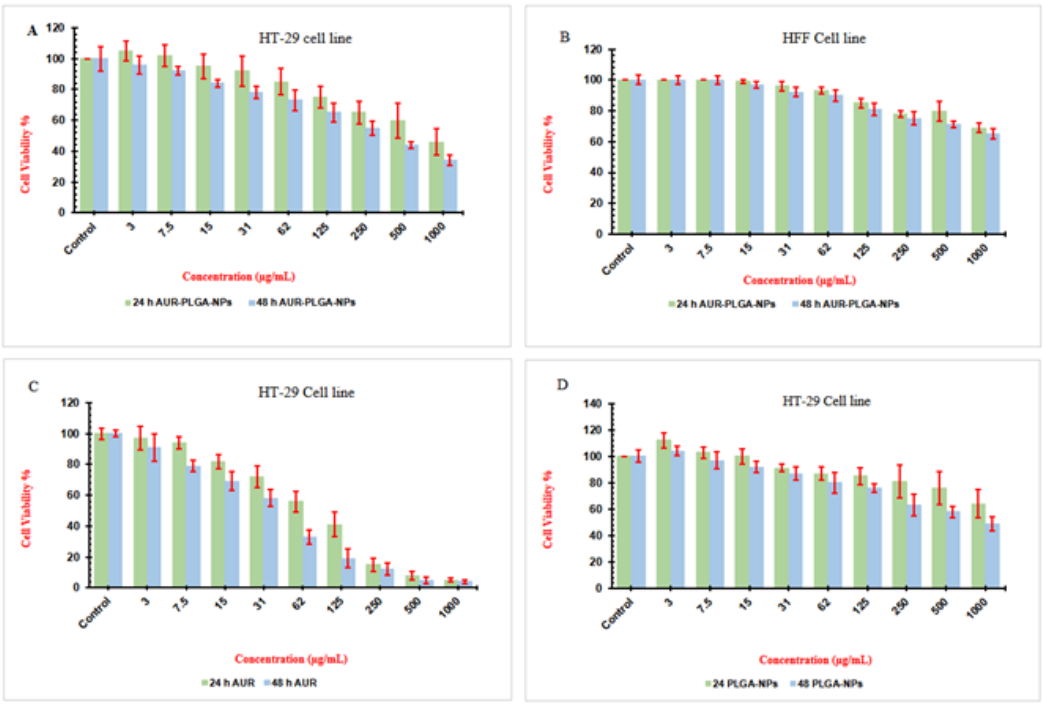

Fig. 4. MTT cell toxicity assay. The Aur-PLGA-NPs at different doses were incubated with HT-29 cancer cells (24 and 48 hr) and showed concentration- and time-dependent cytotoxicity against these cells. The IC50 value was equal to 250 µg/mL. Different doses of Au-PLGA-NPs were incubated with HFF normal cells (24 and 48 hr), showing cytotoxicity against these cells

PLGA-NPs against HT29 cancer cells at 24 and 48 hr after treatment. Examination of normal cells (i.e., HFF) indicated that the nanoparticles had low effect on the viability of these cells (Fig. 4B). However, Aur-PLGA-NPs had significant toxicity against cancer cells, reducing their viability in a concentration- and time-dependent manner. We also evaluated the cytotoxicity pattern of PLGA-NPs and bare Aur against HT29 cancer cells at 24 and 48 hr after treatment (Fig. 4C&D). The results indicated that Aur exhibits high toxicity on the examined cells, with viable cell counts dropping below 20% at concentrations of 250 µg/ml. For PLGA-NPs, a dose-dependent cytotoxic effect on the cancer cells was also observed; however, the observed toxicity was lower than that of both bare Aur and Aur-PLGA-NPs. These findings suggest that while PLGA-NPs alone can exert a cytotoxic effect, the incorporation of Aur significantly enhances this effect, making Aur-PLGA-NPs more effective at reducing cancer cell viability. The lower toxicity of PLGA-NPs compared to bare Aur and Aur-PLGA-NPs underscores the importance of the Aur component in driving the anti-cancer effects. This suggests that the intrinsic anti-cancer activity of Aur is retained within the nanoparticle formulation. Interestingly, while PLGA-NPs alone demonstrated a dose-dependent cytotoxic effect, their overall toxicity was lower than both bare Aur and Aur-PLGA-NPs. This finding suggests a synergistic effect between Aur and PLGA within the nanoparticle formulation, potentially due to enhanced cellular uptake, improved intracellular release, or increased stability of Aur when encapsulated within PLGA. Our findings indicate a noteworthy decrease in the toxicity of Aur when encapsulated within the nanostructure compared to its free form. This reduction in toxicity is potentially attributed to the sustained release profile afforded by the nanocarrier. By entrapping Aur within the nanomatrix, its release is controlled and prolonged, leading to a lower systemic exposure to the free drug. This sustained release mechanism could minimize off-target effects on healthy cells in-vivo, enhancing its therapeutic index and safety profile [37, 38]. Further investigation into the in-vivo pharmacokinetics and biodistribution of both free and encapsulated Aur will provide critical insights into the relationship between controlled release and reduced toxicity. These data in similar to previous studies. These similar studies used PLGA for antitumor drug delivery and adjuvant therapy due to their ability to encapsulate and release drugs, as well as passively target tumors [33, 39-41]. Overall, the study demonstrates that Aur-PLGA-NPs are a promising candidate for targeted cancer therapy, offering a potent, selective cytotoxic effect against cancer cells while sparing normal cells. Further studies are needed to explore the mechanisms underlying this selective toxicity and to evaluate the in-vivo efficacy and safety of these nanoparticles. Aur's cytotoxicity highlights it for medical application in the treatment of cancer. The dose-dependent inhibition of Aur was also shown in Ghorbani, et al's study on growth of acute myeloid leukemia [42].

DAPI staining

Furthermore, we investigated possible mechanisms underlying the anti-cancer effects of auraptene-loaded PLGA nanoparticles. Our results indicated that the nanoparticles induced apoptosis in cancer cells (Fig. 5). Apoptosis is one of the mechanisms of cell growth suppression. DAPI is a fluorescent dye that can be used to visualize apoptotic nucleus changes in cells. As displayed in Fig. 4, Aur-PLGA-NPs induced apoptotic changes in the nuclei of treated cells compared to untreated control cells. In a concentration-dependent way, Aur-PLGA-NPs increased nuclear apoptotic bodies and chromatin density in cells, while the cell nucleus in the control group appeared normal. Also, chromatin fragmentation was observed in the cells treated with Aur-PLGA-NPs, showing

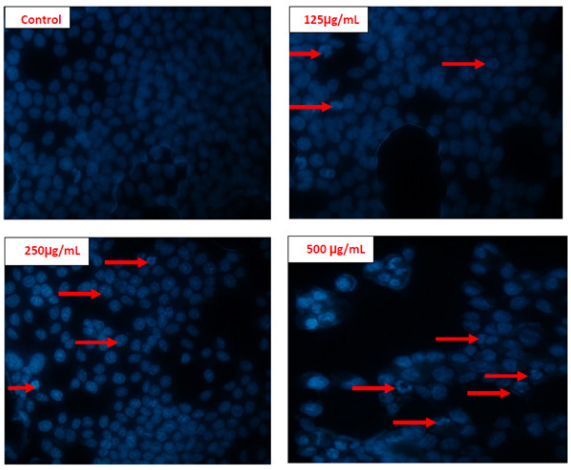

Fig. 5. DAPI staining for monitoring apoptotic nucleus changes in HT-29 cancerous cells exposed to Aur-PLGA-NPs (125, 250, and 500 µg/mL). The cell nucleus in the control group was morphologically normal, but chromatin fragmentation was evident in the cells treated with Aur-PLGA-NP. 40× magnification

that these particles could induce apoptosis in HT-29 cells. Thus, the DAPI staining results revealed significant apoptotic changes in the nuclei of cells treated with Aur-PLGA-NPs compared to the untreated control group. In particular, we observed an increase in nuclear apoptotic bodies and heightened chromatin density in a concentration-dependent manner. These findings align with previous studies that have highlighted the role of chromatin condensation and fragmentation as hallmarks of apoptosis [43, 44]. The observed chromatin fragmentation in HT-29 cells treated with Aur-PLGA-NPs further supports the assertion that these nanoparticles trigger apoptotic pathways, leading to cell death. The mechanisms underlying the apoptosis induced by Aur-PLGA-NPs could involve multiple pathways. One possibility is the activation of caspases, a family of cysteine proteases that play essential roles in the execution phase of apoptosis [45, 46]. Previous studies have shown that PLGA nanoparticles can enhance the delivery of therapeutic agents, leading to increased reactive oxygen species (ROS) production and subsequent activation of the mitochondrial apoptosis pathway [33, 47]. The generation of ROS can disrupt mitochondrial membrane potential, leading to the release of cytochrome c and the activation of caspases, ultimately resulting in apoptosis [48]. Moreover, the concentration-dependent increase in apoptotic bodies suggests a dose-response relationship, which is critical for optimizing the therapeutic efficacy of Aur-PLGA-NPs in cancer treatment. This observation is consistent with other studies that have reported similar dose-dependent effects of nanoparticle-mediated drug delivery systems on apoptosis induction [4, 49]. The development of effective drug delivery systems, such as PLGA nanoparticles, enhances the bioavailability of therapeutic agents like auraptene, which may exhibit limited solubility and stability in physiological conditions [50, 51]. By encapsulating auraptene in PLGA nanoparticles, we not only improve its pharmacokinetic properties but also facilitate targeted delivery to cancer cells, minimizing the adverse effects on normal tissues. In conclusion, our findings suggest that auraptene-loaded PLGA nanoparticles effectively induce apoptosis in HT-29 cancer cells through mechanisms likely involving caspase activation and ROS production. These results highlight the potential of Aur-PLGA-NPs as a promising therapeutic strategy in cancer treatment, warranting further investigation into their efficacy in in vivo models and their applicability in clinical settings.

Flow cytometry assay

Flow cytometry was used to evaluate the apoptotic effects of auraptene-loaded PLGA nanoparticles by measuring Annexin V/PI staining. In a Ca2+-dependent manner, Annexin V binds to membrane phospholipids, with a high binding affinity for phosphatidylserine. In apoptotic cells, Annexin V is expelled out of the cell by being translocated from the inner to the outer leaflet of the plasma membrane, allowing this assay to discern alive cells from necrotic ones, as well as cells in early apoptosis from those in late apoptotic stages. According to our results, most HT-29 cells exposed to the different concentrations of Aur-PLGA-NPs were either necrotic (Annexin V negative/PI positive) or late apoptotic (double positive). As shown in Fig. 6 while HT-29 cells treated with Aur-PLGA-NPs underwent apoptosis, the viability of control cells reached 90.3%. After 48 hr of exposure to Aur-PLGA-NPs, the ratio of Annexin V-FITC-positive HT-29 cells increased gradually from 6.4% to 70.4%. Our results indicated

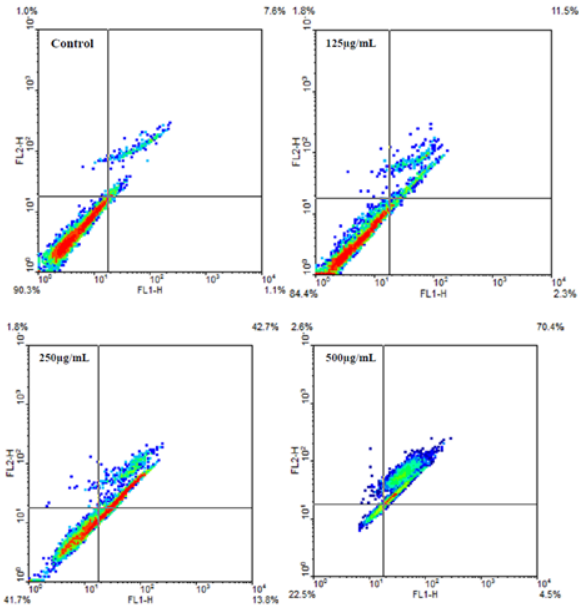

Figure 6. Annexin V-FITC staining. Treatment with Aur-PLGA-NPs induced apoptosis in HT-29 cells (24 hr), evidenced by an increase in the ratio of Annexin V-FITC-positive cells over time. At the concentrations of 125, 250, and 500 µg/mL, the percentages of late apoptotic cells were recorded as 11.5%, 42.7%, and 70.4%, respectively

that the nanoparticles induce apoptosis in cancer cells. Flow cytometry analysis can be conducted to evaluate the apoptosis-inducing properties of the Auraptene-loaded PLGA nanoparticles by measuring Annexin V/PI staining. The findings from the flow cytometry analysis underscore the pro-apoptotic effects of auraptene-loaded PLGA nanoparticles on HT-29 colorectal cancer cells. The use of Annexin V/PI staining provided a clear distinction between viable, early apoptotic, late apoptotic, and necrotic cells, facilitating the assessment of the apoptotic process induced by Aur-PLGA-NPs. The translocation of phosphatidylserine to the outer leaflet of the plasma membrane is a hallmark of early apoptosis and serves as a signal for phagocytic cells to recognize and clear dying cells [52]. The significant increase in Annexin V-FITC-positive cells from 6.4% to 70.4% after 48 hr of treatment with Aur-PLGA-NPs indicates a robust induction of apoptosis, suggesting that these nanoparticles effectively trigger apoptotic pathways in HT-29 cells. This is particularly relevant, as the ability to induce apoptosis in cancer cells is a key strategy in cancer therapy. The high percentage of necrotic cells observed alongside late apoptotic cells may suggest that the treatment with Aur-PLGA-NPs not only stimulates apoptosis but may also lead to secondary necrosis if the apoptotic process is overwhelmed or if the cells fail to undergo the apoptotic program in a controlled manner [53]. This dual observation highlights the complexity of cell death mechanisms in response to nanoparticle treatment. Additionally, the negligible impact on the viability of control cells (90.3%) suggests that Aur-PLGA-NPs selectively target cancer cells while sparing normal cells, which is a desirable characteristic for therapeutic agents aimed at minimizing side effects. This selectivity is crucial for achieving effective cancer treatment with minimal toxicity. In conclusion, our results demonstrate that auraptene-loaded PLGA nanoparticles effectively induce apoptosis in HT-29 cells, as evidenced by the significant increase in Annexin V-positive cells. These findings support the potential of Aur-PLGA-NPs as a promising therapeutic strategy in the treatment of colorectal cancer, warranting further investigation into their *in-vivo* efficacy and underlying molecular mechanisms.

Expression of apoptotic genes

To further investigate apoptosis, three pro-apoptotic genes, BAX, caspase 3, and caspase 9, were quantified. The results showed that the nanoparticles had a significant effect on BAX gene expression, which proved upregulation with an increase in the concentration of Aur-PLGA-NPs. Compared to the control group, the cells treated with 125, 250, and 500 µg/mL of Aur-PLGA-NPs significantly increased the expression of caspase 3 and 9 genes, with a more prominent effect on caspase 3 (Fig. 7). Gene expression analysis by real-Time –PCR confirmed that the nanoparticles could upregulate the expression of pro-apoptotic markers and caspase enzymes, providing further insights into the efficacy of the nanoparticles in inhibiting cancer cell proliferation and inducing programmed cell death.

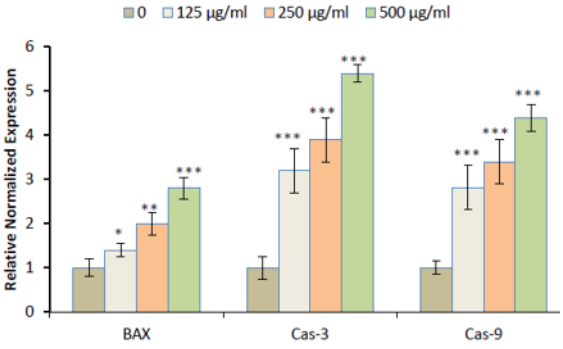

Fig 7. Apoptotic genes' expression (BAX, caspase3, and caspase 9). Aur-PLGA-NPs dose-dependently increased the expression of these apoptotic genes compared to the control group

The use of PLGA as a carrier for auraptene also offers advantages in terms of biocompatibility and biodegradability [54]. PLGA is a FDA-approved polymer widely used in drug delivery systems [55] as it undergoes hydrolysis in the body, leading to the gradual release of the encapsulated drug. The biodegradability of PLGA nanoparticles ensures the elimination of the carrier from the body without causing any long-term toxicity [56].

CONCLUSION

The synthesis of PLGA nanoparticles loaded with auraptene seemed to be a promising strategy for the development of effective anti-cancer therapies. The encapsulation of auraptene within PLGA nanoparticles enhances its stability, controlled release, cellular uptake, and anti-cancer effects. The biocompatibility and biodegradability of PLGA nanoparticles further contribute to their potential clinical translation. Future studies should focus on the *in-vivo* evaluation and optimization of this nanoparticle formulation to ensure the

effective delivery of auraptene to tumors while minimizing systemic toxicity.

ACKNOWLEDGMENTS

The authors would like to thank the department of biology Mashhad Branch of the Islamic Azad University for supporting chemicals and laboratory facilities.

FUNDING

This study received no particular grant from any source.

CONFLICT OF INTEREST

The authors have no conflicts of interest to declare.

REFERENCES

1. Ahmadi R, Es-haghi A, Zare-Zardini H, Taghavizadeh Yazdi ME. Nickel oxide nanoparticles synthesized by Rose hip extract exert cytotoxicity against the HT-29 colon cancer cell line through the caspase-3/caspase-9/Bax pathway. Emergent Mater 2023; 6(6): 1877-1888.
2. Alabyadh T, Albadri R, Es-Haghi A, Yazdi MET, Ajalli N, Rahdar A, et al. ZnO/CeO_2 Nanocomposites: Metal-Organic Framework-Mediated Synthesis, Characterization, and Estimation of Cellular Toxicity toward Liver Cancer Cells. J Funct Biomater. 2022; 13(3): 139.
3. Alvi M, Yaqoob A, Rehman K, Shoaib SM, Akash MSH. PLGA-based nanoparticles for the treatment of cancer: Current strategies and perspectives. AAPS Open. 2022; 8(1): 12.
4. Bibak B, Shakeri F, Barreto GE, Keshavarzi Z, Sathyapalan T, Sahebkar A. A review of the pharmacological and therapeutic effects of auraptene. Biofactors. 2019; 45(6): 867-879.
5. Calzoni, E, Cesaretti A, Polchi A, Di Michele, A, Tancini B, Emiliani C. Biocompatible polymer nanoparticles for drug delivery applications in cancer and neurodegenerative disorder therapies. J Funct Biomater. 2019; 10(1): 4.
6. Chatterjee M, Chanda N. Formulation of PLGA nano-carriers: specialized modification for cancer therapeutic applications. Mater Adv. 2022; 3(2): 837-858.
7. Chaurio RA, Janko C, Muñoz LE, Frey B, Herrmann M, et al. Phospholipids: Key players in apoptosis and immune regulation. Molecules. 2009; 14(12): 4892-4914.
8. Che Marzuki NH, Wahab RA, Abdul Hamid M. An overview of nanoemulsion: Concepts of development and cosmeceutical applications. Biotechnol Biotechnol Equip. 2019; 33(1): 779-797.
9. Choi JS, Seo K, Yoo JW. Recent advances in PLGA particulate systems for drug delivery. J Pharm Investig. 2012; 42: 155-163.
10. Donini M, Gaglio SC, Laudanna C, Perduca M, Dusi S. Oxyresveratrol-Loaded PLGA nanoparticles inhibit oxygen free radical production by human monocytes: Role in nanoparticle biocompatibility. Molecules. 2021; 26(14): 4351.
11. Ebrahimi S, Mostafavi-Pour Z, Khazaei M, Nazari SE, Jamshidi ST, Soukhtanloo M. Suppression of metastasis by citrus auraptene in a mouse model of colorectal cancer. Rev Bras Farmacogn. 2023; 33(1): 182-190.
12. Elmore, S. Apoptosis: a review of programmed cell death. Toxicol Pathol. 2007; 35(4): 495-516.
13. Es-haghi A, Taghavizadeh Yazdi ME, Sharifalhoseini M, Baghani M, Yousefi E, Rahdar A, Baino F. Application of response surface methodology for optimizing the therapeutic activity of ZnO Nanoparticles biosynthesized from aspergillus niger. Biomimetics. 2021; 6(2): 34.
14. Eslamieh-Ei FM, Sharifimoghaddammood N, Poustchi Tousi SA, Basharkhah S, Mottaghipisheh J, Es-Haghi A, et al. Synthesis and its characterisation of selenium/silver/chitosan and cellular toxicity against liver carcinoma cells studies. Nat Prod Res. 2023; 1-9.
15. Farhangfar SD, Fesahat F, Zare-Zardini H, Dehghan-Manshadi M, Zare F, Miresmaeili SM, et al. *In vivo* study of anticancer activity of ginsenoside Rh2-containing arginine-reduced graphene in a mouse model of breast cancer. Iran J Basic Med Sci. 2022; 25(12): 1442.
16. Farhangfar SD, Fesahat F, Zare-Zardini H, Dehghan-Manshadi M, Zare F, Miresmaeili SM, et al. Behavioral studies of mice with breast cancer after treatment with new anticancer agent, Rh2-containing arginine-graphene. Academia J. 2023; 38(1):63-65
17. Fiorito S, Preziuso F, Sharifi-Rad M, Marchetti L, Epifano F, Genovese S. Auraptene and umbelliprenin: A review on their latest literature acquisitions. Phytochem Rev. 2022; 21:317-326.
18. Ghorbani M, Soukhtanloo M, Farrokhi AS, Hassanian SM, Ghorbani F, Afshari AR et al. Auraptene-induced cytotoxic effects in acute myeloid leukemia cell lines. Med Oncol, 2023; 40(8): 231.
19. Gomes dos Reis L, Lee WH, Svolos M, Moir LM, Jaber R, Windhab N, et al. Nanotoxicologic effects of PLGA nanoparticles formulated with a cell-penetrating peptide: Searching for a safe pDNA delivery system for the lungs. Pharmaceutics. 2019; 11(1): 12.
20. Grabowski N, Hillaireau H, Vergnaud-Gauduchon J, Nicolas V, Tsapis N, Kerdine-Römer S, et al. Surface-modified biodegradable nanoparticles' impact on cytotoxicity and inflammation response on a co-culture of lung epithelial cells and human-like macrophages. J Biomed Nanotech. 2016; 12(1): 135-146.
21. Green DR, Kroemer G. The pathophysiology of mitochondrial cell death. Science. 2004; 305(5684): 626-629.
22. Gupta P, Singh A, Verma AK, Kant S, Pandey AK, et al. The anti-tumor and immunomodulatory effects of PLGA-based docetaxel nanoparticles in lung cancer: The potential involvement of necroptotic cell death through reactive oxygen species and calcium build-up. Vaccines (Basel). 2022; 10(11):1801.
23. Haghi Karamallah M, Alemi A, Ahmad Hosseini S, Tahery N, Radmanesh E, Malihi R, et al. Co-encapsulation of curcumin and paclitaxel using non-ionic surfactant based nanovesicles suppresses growth of ovarian carcinoma through the inhibition of nuclear factor κB and AKT1. Chemistry Select. 2024; 9(2): e202304221.
24. Honary S, Zahir F. Effect of zeta potential on the properties of nano-drug delivery systems-a review (Part 2). Trop J Pharm Res. 2013; 12(2): 265-273.
25. Jaiswal M, Dudhe R, Sharma P. Nanoemulsion: An advanced mode of drug delivery system. 3 Biotech. 2015; 5: 123-127.
26. Khalil Abad MH, Nadaf M, Taghavizadeh Yazdi ME. Biosynthesis of ZnO. Ag_2O_3 using aqueous extract of Haplophyllum obtusifolium: Characterization and cell toxicity activity against liver carcinoma cells. Micro Nano

Lett. 2023; 18(6): e12170.
27. Kızılbey K. Optimization of rutin-loaded PLGA nanoparticles synthesized by single-emulsion solvent evaporation method. Acs Omega. 2019; 4(1): 555-562.
28. Laxmi M, Bhardwaj A, Mehta S, Mehta A. Development and characterization of nanoemulsion as carrier for the enhancement of bioavailability of artemether. Artif Cells Nanomed Biotechnol. 2015; 43(5): 334-344.
29. Lü JM, Wang X, Marin-Muller C, Wang H, Lin PH, Yao Q, et al. Current advances in research and clinical applications of PLGA-based nanotechnology. Expert Rev Mol Diagn. 2009; 9(4): 325-341.
30. Makadia HK, Siegel SJ. Poly lactic-co-glycolic acid (PLGA) as biodegradable controlled drug delivery carrier. Polymers. 2011; 3(3): 1377-1397.
31. Mehta TA, Shah N, Parekh K, Dhas N, Patel JK. Surface-modified PLGA nanoparticles for targeted drug delivery to neurons. 2019; 33-71.
32. Mobaraki F, Momeni M, Jahromi M, Kasmaie FM, Barghbani M, Yazdi MET, et al. Apoptotic, antioxidant and cytotoxic properties of synthesized AgNPs using green tea against human testicular embryonic cancer stem cells. Process Biochem. 2022; 119: 106-118
33. Mobaraki F, Momeni M, Yazdi MET, Meshkat Z, Toosi MS, Hosseini SM. Plant-derived synthesis and characterization of gold nanoparticles: Investigation of its antioxidant and anticancer activity against human testicular embryonic carcinoma stem cells. Process Biochem. 2021; 111: 167-177.
34. Mohammadzadeh V, Rahiman N, Cabral H, Quader S, Zirak MR, Yazdi MET, et al. Poly-γ-glutamic acid nanoparticles as adjuvant and antigen carrier system for cancer vaccination. J Control Release. 2023; 362: 278-296.
35. Mousavi-Kouhi SM, Beyk-Khormizi A, Amiri MS, Mashreghi M, Hashemzadeh A, Mohammadzadeh V, et al. Plant gel-mediated synthesis of gold-coated nanoceria using ferula gummosa: characterization and estimation of its cellular toxicity toward breast cancer cell lines. J Funct Biomat. 2023; 14(7): 332.
36. Mousavi-Kouhi SM, Beyk-Khormizi A, Amiri MS, Mashreghi M, Yazdi MET. Silver-zinc oxide nanocomposite: From synthesis to antimicrobial and anticancer properties. Ceramics Int, 2021 47(15): 21490-21497.
37. Mousavi-Kouhi SM, Beyk-Khormizi A, Mohammadzadeh V, Ashna M, Es-haghi A, Mashreghi M, et al. Biological synthesis and characterization of gold nanoparticles using Verbascum speciosum Schrad. and cytotoxicity properties toward HepG2 cancer cell line. Res Chem Intermed. 2022; 48(1): 167-178.
38. Paris JL, Baeza A, Vallet-Regí M. Overcoming the stability, toxicity, and biodegradation challenges of tumor stimuli-responsive inorganic nanoparticles for delivery of cancer therapeutics. Expert Opin Drug Deliv. 2019; 16(10): 1095-1112.
39. Rahimi E, Asefi F, Afzalinia A, Khezri S, Zare-Zardini H, Ghorani-Azam A, et al. Chitosan coated copper/silver oxide nanoparticles as carriers of breast anticancer drug: Cyclin D1/P53 expressions and cytotoxicity studies. Inorg Chem Commun. 2023; 111581.
40. Rahimi E, Asefi F, Afzalinia A, Khezri S, Zare-Zardini H, Ghorani-Azam A, et al. Chitosan coated copper/silver oxide nanoparticles as carriers of breast anticancer drug: Cyclin D1/P53 expressions and cytotoxicity studies. Inorg Chem Commun. 2023;, 158: 111581.
41. Ramos AP. Dynamic light scattering applied to nanoparticle characterization. In Nanocharacterization Techniques. 2017; Elsevier.99-110.
42. Razavi MS, Abdollahi A, Malek-Khatabi A, Ejarestaghi, NM, Atashi A, Yousefi N, et al. Recent advances in PLGA-based nanofibers as anticancer drug delivery systems. J Drug Deliv Sci Technol. 2023; 104587.
43. Ruirui Z, He J, Xu X, Li S, Peng H, Deng Z, Huang Y. PLGA-based drug delivery system for combined therapy of cancer: Research progress. Mat Res Express. 2021; 8(12): 122002.
44. Saberian E, Jenča A, Petrášová A, Zare-Zardini H, Ebrahimifar M. Application of Scaffold-Based Drug Delivery in Oral Cancer Treatment: A Novel Approach. Pharmaceutics. 2024; 16(6): 802.
45. Saini RK, Ranjit A, Sharma K, Prasad P, Shang X, Gowda KGM, et al. Bioactive compounds of citrus fruits: A review of composition and health benefits of carotenoids, flavonoids, limonoids, and terpenes. Antioxidants. 2022; 11(2): 239.
46. Serrano-Lotina A, Portela R, Baeza P, Alcolea-Rodriguez V, Villarroel M, Ávila P. Zeta potential as a tool for functional materials development. Catalysis Today. 2023; 423: 113862.
47. Shakerimanesh K, Bayat F, Shahrokhi A, Baradaran A, Yousefi E, Mashreghi M, et al. Biomimetic synthesis and characterisation of homogenouse gold nanoparticles and estimation of its cytotoxity against breast cancer cell line. Mater Technol. 2022; 1-8.
48. Shariatinia Z, Oroujzadeh N. Anticancer drug delivery shuttles based on polyethylene glycol-polylactic acid nanocomposites: Molecular dynamics simulations. J Nanostruct. 2021; 11(2): 347-367.
49. Taghavizadeh Yazdi ME, Amiri MS, Darroudi M. Biopolymers in the synthesis of different nanostructuresavizadeh. In book: Reference Module in Materials Science and Materials EngineeringPublisher: Elsevier
50. Taghavizadeh Yazdi ME, Darroudi M, Amiri MS, Zarrinfar H, Hosseini HA, Mashreghi M, et al. Antimycobacterial, anticancer, antioxidant and photocatalytic activity of biosynthesized silver nanoparticles using Berberis Integerrima. Iran J Sci Technol. 2022; 46(1): 1-11.
51. Taghavizadeh Yazdi ME, Qayoomian M, Beigoli S, Boskabady MH. Recent advances in nanoparticle applications in respiratory disorders: A Review. Front Pharmacol. 2023; 14: 1059343.
52. Yetisgin AA, Cetinel S. Therapeutic nanoparticles and their targeted delivery applications. 2020; 25(9): doi:10.3390/molecules25092193
53. Yusuf A, Almotairy ARZ, Henidi H, Alshehri OY, Aldughaim MS. Nanoparticles as drug delivery systems: a review of the implication of nanoparticles' physicochemical properties on responses in biological systems. Polymers. 2023; 15(7): 1596.
54. Zarharan H, Bagherian M, Rokhi AS, Bajgiran RR, Yousefi E, Heravian P, et al. The anti-angiogenesis and antioxidant activity of chitosan-mediated synthesized selenium-gold nanostructure. Arab J Chem. 2023; 16(7): 104806.
55. Zhang D, Liu L, Wang J, Zhang H, Zhang Z, Xing G, et al. Drug-loaded PEG-PLGA nanoparticles for cancer treatment. Front Pharmacol. 2022; 13: 990505.
56. Zhang D, Liu L, Wang J, Zhang H, Zhang Z., Xing G., et al. Drug-loaded PEG-PLGA nanoparticles for cancer treatment. Front Pharmacol. 2022; 13: 990505.